JOURNAL OF MATERIALS SCIENCE **37** (2002) 3075 – 3084

Load controlled low cycle fatigue of $[0]_8$ Sigma fibre reinforced titanium matrix composite

M. P. THOMAS
Structures and Materials Centre, QinetiQ plc, Cody Technology Park, Farnborough, Hampshire, GU14 OLX, UK
E-mail: mpthomas@QinetiQ.com

Fibre reinforced titanium matrix composites (TMCs) are being considered for use in future aeronautical gas-turbine compressor discs. Low cycle fatigue is thought to be one of the mechanisms most damaging to such a component. Here, the low cycle fatigue behaviour of Ti-6-4, reinforced with SM1140+ fibre, is investigated over the temperature range 22°C to 600°C. SN curves have a characteristic "S" shape and can be split into three regions. Fractography, acoustic emission monitoring and cyclic strain recording have elucidated damage mechanisms in each region. In region I (high cyclic stress) damage is caused by matrix creep, that leads to fibre failure. In region III (low cyclic stress), the predominant damage mechanism is matrix crack growth. Cracks initiate at surface machining damage and grow, bridged by intact fibres, into the bulk. The matrix crack growth transfers stress to fibres, eventually causing them to fail in overload, resulting in specimen failure. In region II (intermediate cyclic stress) damage is by a combination of the mechanisms observed in regions I and III. Comparison of Ti-6-4/SM1140+ with Ti-6-4/SCS-6 shows that fatigue lives are similar in regions II and III. In region I it is possible that Ti-6-4/SM1140+ has inferior lives to Ti-6-4/SCS-6.

1. Introduction

An increase in thrust to weight (T/W) ratio is required to achieve the performance targets defined for future military aircraft. Whilst advances in turbo-machinery will contribute to the attainment of these targets, the overall performance targets will not be met without the introduction of advanced materials. One such material is SiC fibre reinforced titanium matrix composite (TMC). Since the reinforcing fibres are ceramic, TMC mechanical properties can be maintained at temperatures significantly above those that monolithic Ti alloys can withstand. The relatively low density of TMC also means that this class of material has good specific properties, which can lead to a reduction in component weight. This makes them candidates for several components in future aeronautical gas-turbine engines, the most promising of which is the compressor disc. Within the disc the TMC would be a unidirectionally reinforced hoop around the rim.

During operation, disc components are subject to two types of fatigue, high cycle (vibrational) fatigue (HCF) due to the disc rotation and low cycle fatigue (LCF) due to the change in stress level from stand-still to operational speed. It is widely thought that LCF is more damaging to the disc than HCF.

Previously published work on tension-tension low cycle fatigue has been limited to TMCs reinforced with the Textron SCS series of fibres. With a number of other fibres now commercially available, it is important to characterise the mechanical properties of a wide range of TMCs and to compare and contrast the fibre types.

2. Materials and testing procedure

The TMC is a Ti-6-4 (Ti-6A1-4V) matrix reinforced with DERA Sigma SM1140+ carbon coated SiC fibre. 8 ply TMC panels were fabricated at DERA Sigma, via the fibre-foil route. Fibre volume fraction was nominally 0.34. The microstructure of the TMC has been investigated in detail elsewhere [1]. Following the recommendations of previous standardisation work [2] two $[0]_8$ specimen geometries were used. For room temperature tests the DERA dogbone specimen was used, whilst for elevated temperature tests, simple parallel sided specimens, 150 mm × 10 mm were used.

Low cycle fatigue tests were performed under load control, at a frequency of 0.1 Hz, stress ratio, R, of 0.1 and with a triangular waveform. All tests were performed in air. Strain was measured during each test using a Mayes capacitance extensometer with a gauge length of 20 mm. The two extensometer arms had cylindrical ceramic end contacts. The long arms were mounted on the specimens, through holes in the furnace, by means of pressure springs. Analysis of failed specimens showed that the extensometer contacts did not cause premature fatigue crack initiation.

Acoustic emission was monitored in each test using a grip-mounted sensor in conjunction with a 300 kHz–1 MHz filter. This filter range is most suitable for detecting both fibre and interfacial failure [3].

The gain on the acoustic emission equipment was set so that only the highest energy and amplitude events, indicative of fibre failure [4, 5], were detected. Since these events predominately occur near the peak stress of the fatigue cycle [5] a voltage gate was utilised so that acoustic signals were only detected when the cyclic stress was above its mean value.

It has recently been proposed that many cracks seen on polished sections of elevated temperature fatigue specimens are, in fact, due to the polishing procedure and not the test [6]. Matrix creep during elevated temperature fatigue can result in the post-test residual stress in the fibres becoming tensile, allowing easy fibre fracture during the polishing process. For this reason, specimens that were to be examined optically were subjected to a heat treatment of eight hours at 600°C in a vacuum furnace followed by an overnight cool under vacuum. This relieves any tensile stress in the fibres, which should reduce the amount of fibre cracking during polishing [6]. When polished sections were prepared and examined in the optical microscope, however, no difference in the amount of fibre cracking was observed between heat treated and as-tested specimens. Matrix cracking, though, could be observed more easily in the heat-treated specimens. The rate of cooling during the stress-relieving heat treatment may have been sufficiently great to generate a small tensile residual stress in the matrix in the fibre direction, which would act to open up matrix fatigue cracks.

3. S-N behaviour

The LCF data for the Ti-6-4/SM1140+ are plotted as S-N curves in Fig. 1. All the TMC fatigue curves have a

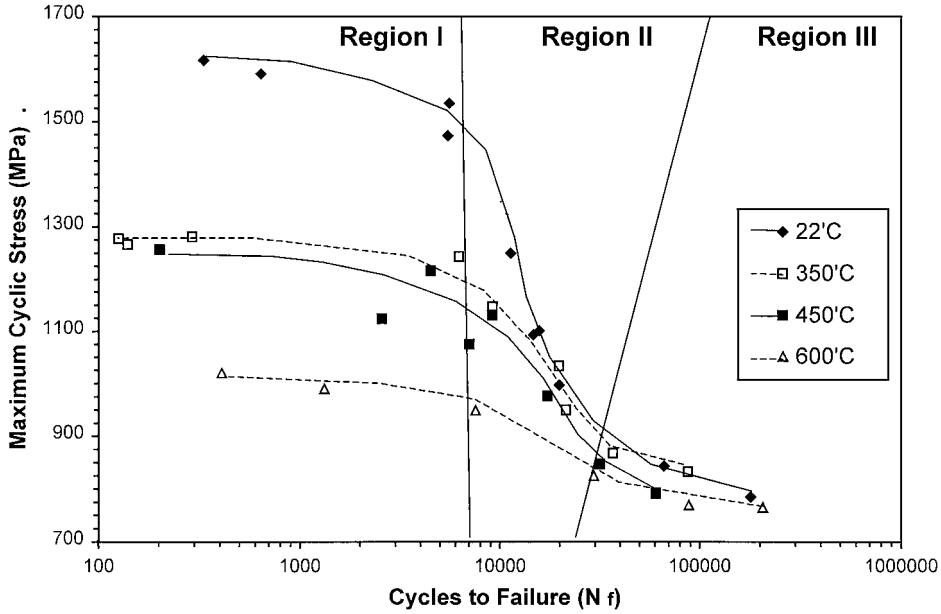

Figure 1 S-N curves for Ti-6-4/SM1140+ TMC.

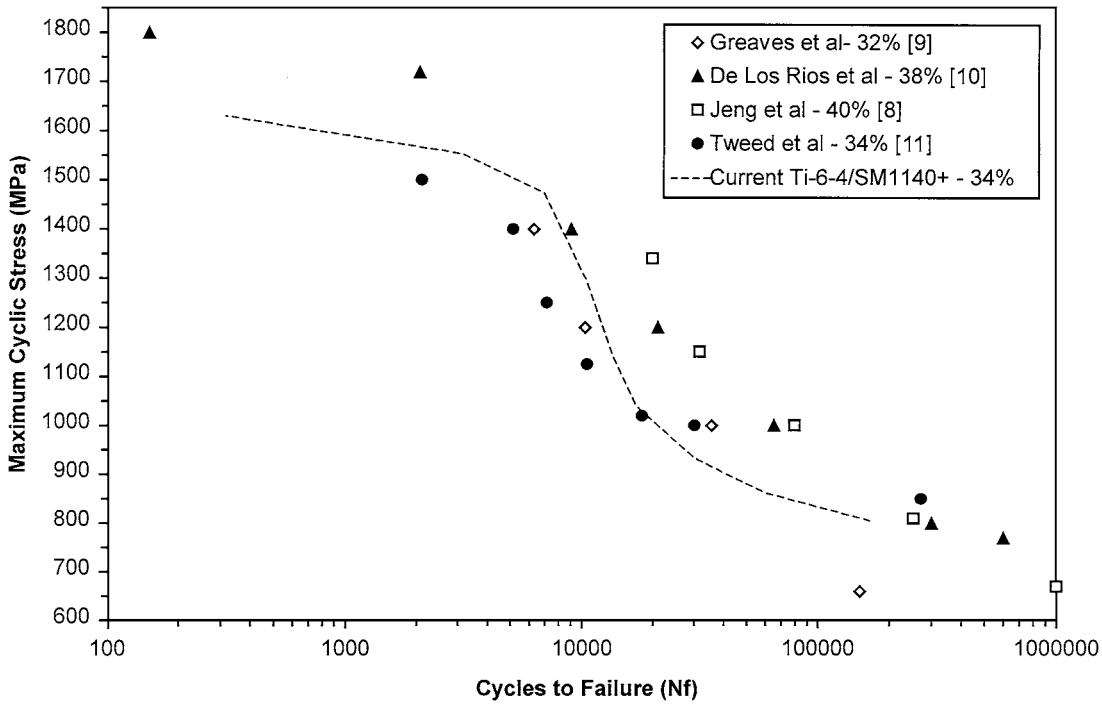

Figure 2 Comparison of S-N curves of Ti-6-4/SM1140+ and Ti-6-4/SCS-6, at room temperature.

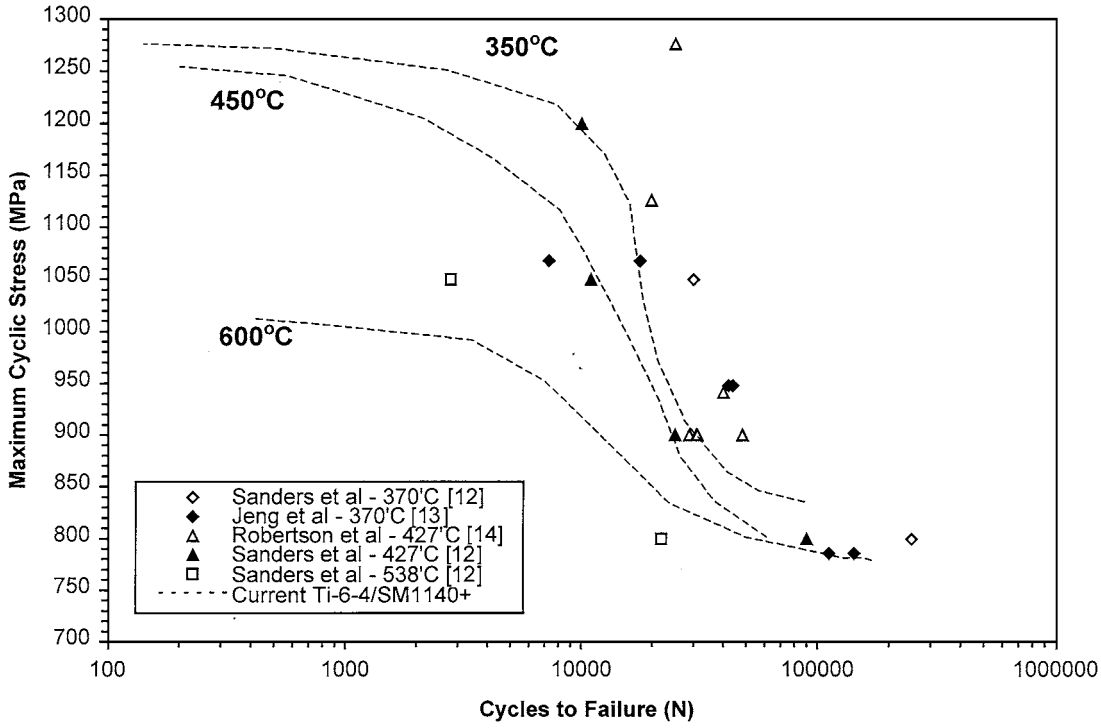

Figure 3 Comparison of elevated temperature S-N curves of Ti-6-4/SM1140+ and Ti-6-4/SCS-6.

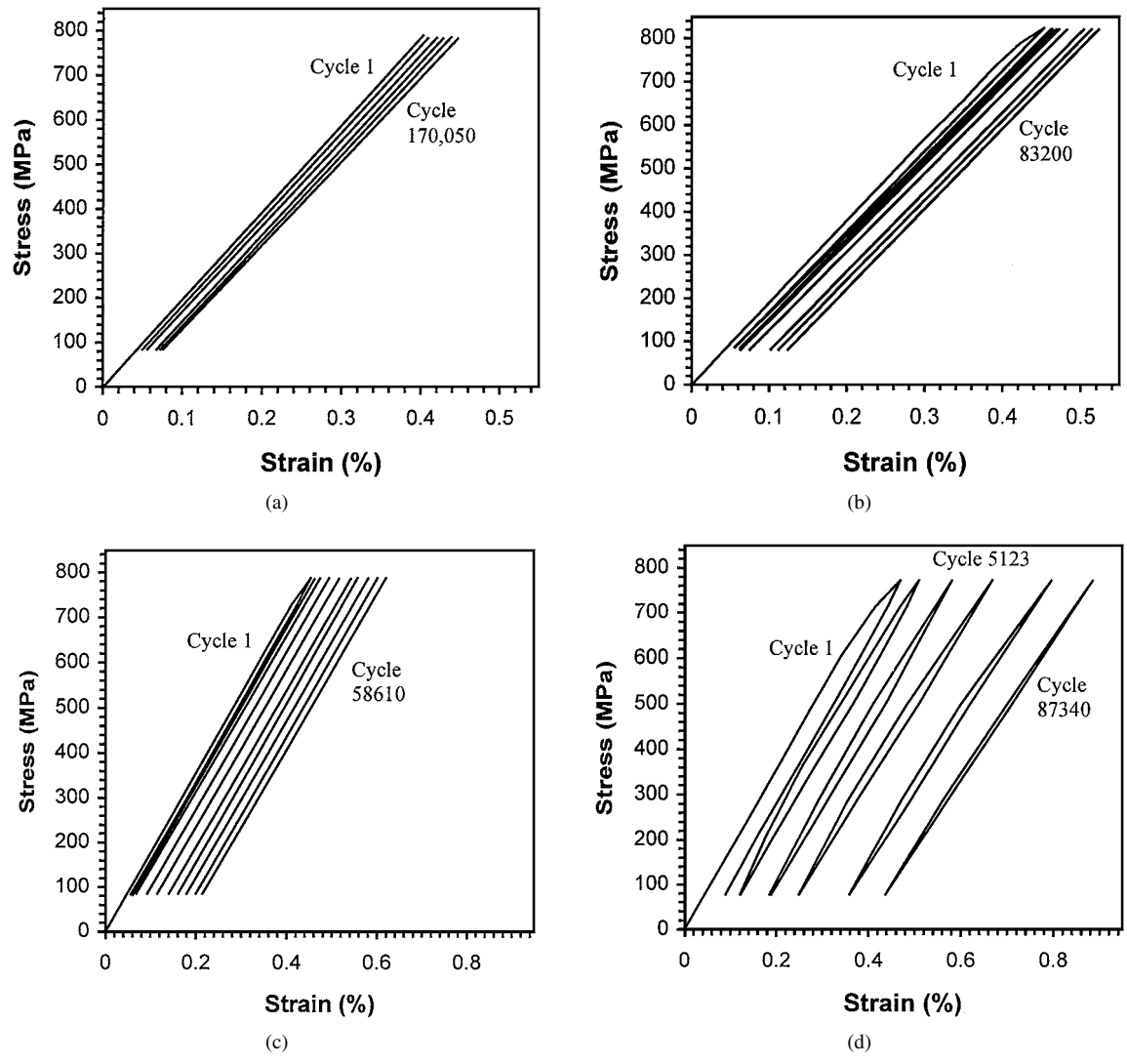

Figure 4 Comparison of cyclic stress-strain curves in Region III of the S-N curve. (a) 22°C, (b) 350°C, (c) 450°C, (d) 600°C.

characteristic "S" shape. Previous work has shown that the S curve can be split into three distinct regions, as shown on Fig. 1, in each of which damage development occurs by distinctly different mechanisms [7]. The observation of these mechanisms has previously been limited, however, to TMCs reinforced with Textron fibres. Section 4 will assess whether the same mechanisms occur in the current SM1140+ reinforced TMC.

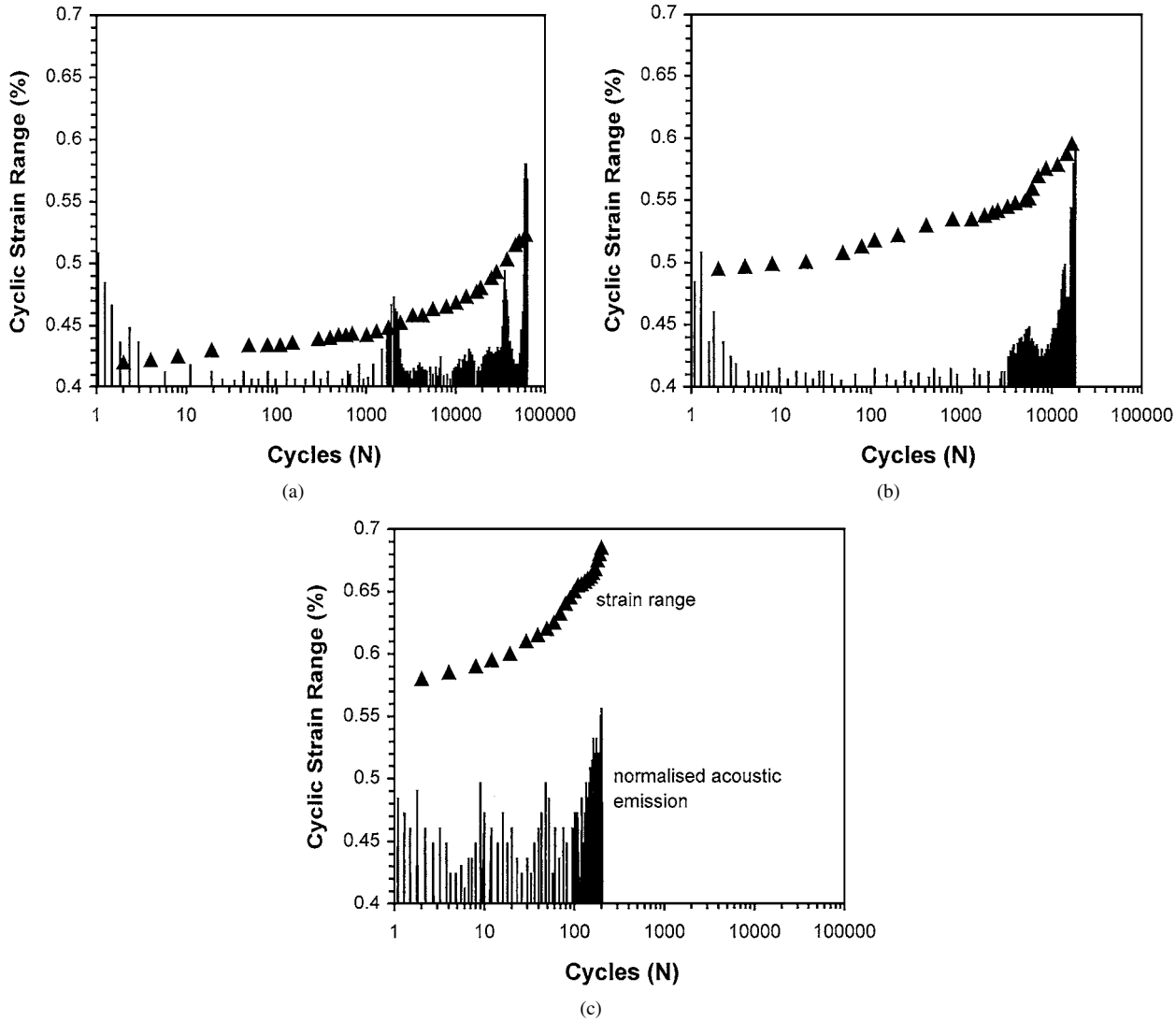

Figure 5 Variation in strain range, and acoustic emission, with fatigue cycle (450°C, but all temperatures were similar). (a) Region III; (b) Region II; (c) Region I.

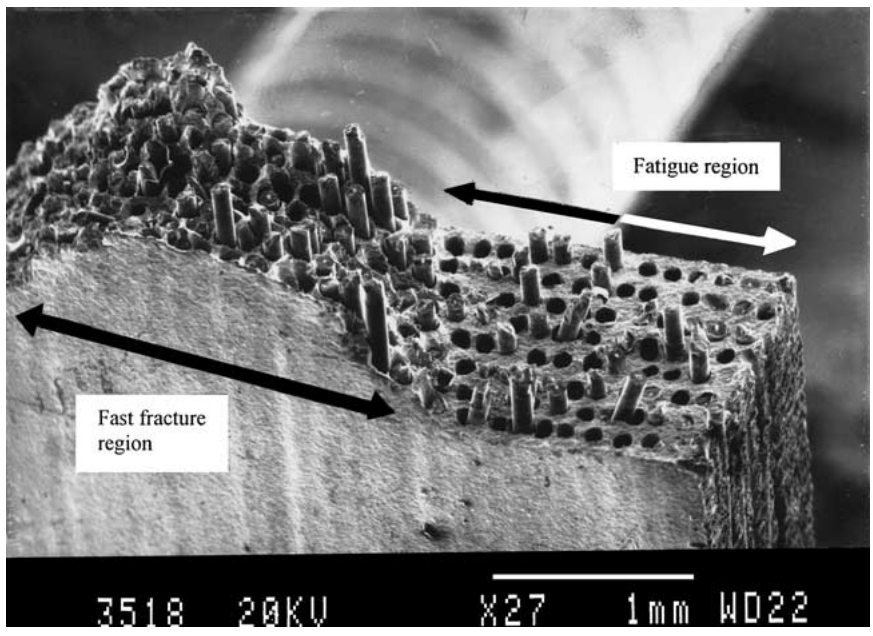

Figure 6 Contrasting topography of fatigue and fast fracture regions.

Fig. 2 compares the current room temperature data with previously reported data for Ti-6-4 reinforced with SCS-6 fibres [8–11]. The SCS-6 based TMC data were obtained at the higher frequency of 10 Hz. It has been shown, however, that fatigue lives of Ti-6-4 based TMC are not affect by frequency below 400°C, in the range 0.01 Hz to 10 Hz [12]. It is sound, therefore, to compare these data sets. If the different fibre contents of each data set is kept in mind (noted on Fig. 2), there is no significant difference in the fatigue performance of Ti-6-4 reinforced with either Sigma SM1140+ or SCS-6 fibres, at room temperature.

Fig. 3 presents a similar comparison between Sigma SM1140+ and SCS-6 reinforced Ti-6-4, at elevated temperature [12–14]. All data is from TMCs with similar fibre volume fractions. At temperatures above 400°C the frequency of testing is expected to affect the fatigue performance [12, 15]. Thus, the data of Jeng *et al*. [13] and Robertson *et al*. [14] would be expected to lie to the right of the current Ti-6-4/SM1140+ data, all else being equal, due to the higher testing frequencies used in those studies. The data of Sanders *et al*. in Fig. 3 [12] was obtained at the same frequency as the current data but at the lower stress ratio, R, of 0.05. A recent study has shown that although decreasing the stress ratio reduces fatigue life in the range $R = 0.5$, through 0.1 and 0 to $R = -1$ [16], the difference when testing at $R = 0.1$ and $R = 0.05$ is likely to be minimal. It is valid, therefore, to compare the data of [12] to the current data.

Keeping in mind the observations in the previous paragraph, and the slightly different temperatures of test between the Ti-6-4/SM1140+ and literature data, it appears that the fatigue performance of Ti-6-4/SM1140+ is comparable to that of Ti-6-4/SCS-6 at low to intermediate stresses (i.e., Regions II and III). At high cyclic stresses (Region I), however, the fatigue lives in Ti-6-4/SM1140+ may become inferior to those of Ti-6-4/SCS-6. In this region TMC failure is thought to be dominated by fibre failure. Sigma SM1140+ is known to have a lower tensile strength than SCS-6, with literature means of 3260 MPa and 3640 MPa respectively [17–20]. The lower fatigue lives of the Ti-6-4/SM1140+ TMC in region I may, thus, be due to the lower strength of the SM1140+ fibre. Differences in interfacial reaction zone thickness and interfacial bond strength between these two Ti-6-4 TMCs may also contribute to differences in their region I fatigue performance [21].

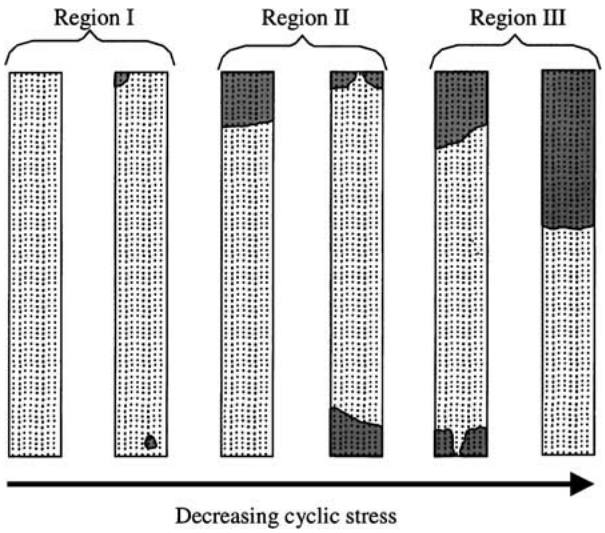

Figure 7 Schematic diagram of variation in matrix fatigue crack size with applied cyclic stress. (350°C shown).

4. Cyclic stress-strain behaviour and damage development

4.1. Region III behaviour

Fig. 4 compares the cyclic stress-strain curves at each temperature in region III. The unloading moduli in the first cycle at each temperature are the same as the loading moduli, indicating that the non-linearity during load up is not caused by internal damage. The permanent plastic strain observed at the end of the first cycle in the

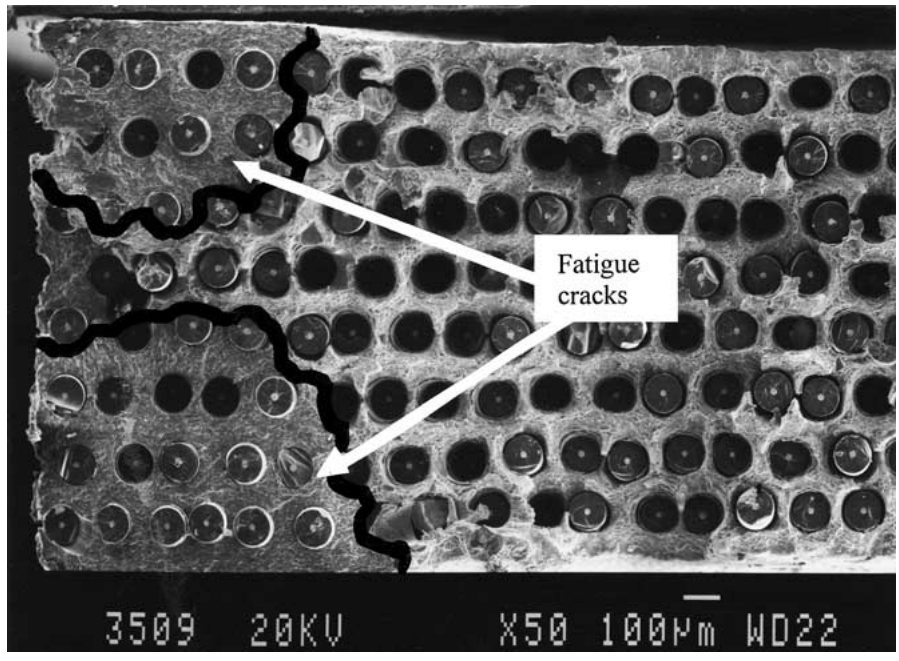

Figure 8 Matrix crack initiation at corners of machined edges.

tests at elevated temperature indicates that non-linearity during load-up was due to plastic matrix yielding [22–24]. Not surprisingly, the magnitude of the retained plastic strain increases with temperature, due to the decreasing strength of the matrix material.

Ratchetting (an increase in maximum and minimum cyclic strains) is observed at all temperatures, in contrast with previous work that showed no ratchetting at room temperature [25]. At elevated temperature this ratchetting is due to creep of the matrix [12, 25]. The ratchetting occurs to a greater extent as the temperature increases, due to the reduction in matrix creep resistance, as has been observed in Ti-15-3/SCS-6 TMC [26]. It is suggested that ratchetting at room temperature is due to matrix slip band initiation at fibre/matrix interfacial stress concentrations, aided by the high matrix tensile residual stress [27].

Fig. 5a presents plots of the variation in cyclic strain range, together with normalised acoustic emission response for a representative specimen in region III. In all tests there is a significant amount of acoustic activity in the first one to three cycles, which quickly drops to background level. It is suggested that this is caused by the failure of surface fibres which have been damaged during the specimen machining process, as the magnitude and period of this acoustic activity is similar at all temperatures [25, 28]. The initial acoustic activity was not due to the settling in or slipping of the specimen in the grips, since previous work on monolithic Ti-6-4 specimens has not shown this activity [29].

It has previously been suggested that an initial increase in strain range is due to random fibre failure [25]. In that work, the random fibre failure continued for approximately 100 cycles before petering. In the current work, however, there is no evidence, through acoustic monitoring, of a period of random fibre failures, beyond the failure of surface damaged fibres in cycles 1 to 3. It is suggested that the slow increase in strain range over the greater portion of fatigue life, is due to matrix creep [25] and the initiation and growth of matrix cracks. Fractographic examinations were performed to investigate matrix crack growth. Matrix fatigue regions could be easily distinguished due to the flatness of failure in those regions. By contrast, the fast fracture regions were extremely rough (Fig. 6). Steps, occasionally seen in the fatigue regions were caused by the intersection of two fatigue cracks. Fig. 7 presents schematic diagrams of the extent of matrix cracking in the current specimens. Matrix cracks in region III grow to a large size at temperatures below 600°C and these will, almost certainly, have a deleterious effect on specimen stiffness and strain range [12]. At the upper temperature of 600°C matrix crack growth is limited, presumably because the low strength of the matrix at this temperature means that matrix creep is the primary deformation mechanism. Certainly, tests at 600°C show the greatest amount of ratchetting (Fig. 4d).

It is clear from Fig. 7 that, in all fatigue regions, matrix cracks initiate almost exclusively at the corners of the machined edges of specimens. Fig. 8 illustrates this crack initiation site. Surface initiation of matrix cracks, particularly from fibres damaged during machining, is commonly observed in TMCs in region III [9, 12, 23, 28, 30, 31]. As well as the failure crack, optical microscopy revealed that many surface initiated cracks occurred away from the final fracture surface. These ranged from a few microns deep to several fibre plies deep (Fig. 9). In all cases the cracks passed around fibres leaving the intact fibres to bridge the crack, as is commonly observed in SCS-6 reinforced TMCs [13, 26, 30, 32–35].

Previous work on as-received Ti-15-3/SCS-6 shows large amounts of fibre/matrix debonding where a matrix crack meets a fibre [8, 33, 36, 37]. This is linked to interfacial chemistry and bond strength, since heat treatment was observed to dramatically reduce this

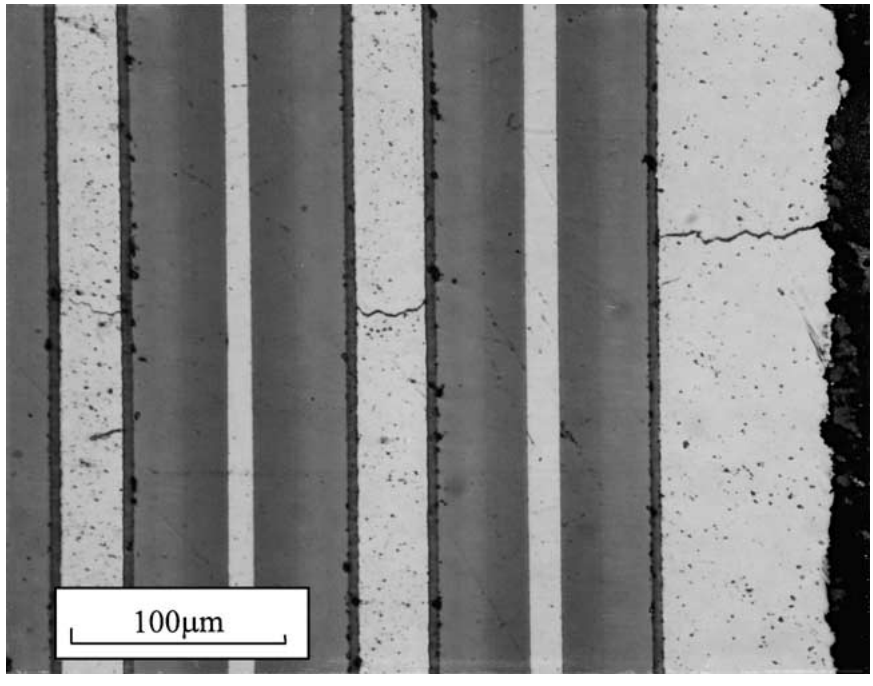

Figure 9 Surface initiated matrix crack passing around intact fibres.

debonding in Ti-15-3/SCS-6 [8]. The effect of bond strength and interfacial morphology on debonding is the subject of current study [38]. In the current Ti-6-4/SM1140+, very limited fibre/matrix debonding is observed (Fig. 9), agreeing with work on Ti-6-4/SCS-6 [8, 12]. This may infer a higher interfacial bond strength than in Ti-15-3/SCS-6.

Initiation of fatigue cracks within the bulk of specimens was only observed once in region III. This occured in the specimen tested at 450°C and 792 MPa (Fig. 10). In this case, the internal fatigue crack initiated at a bulk defect where three fibres were touching. This specimen gave a fatigue life of 60360 cycles when, from the graphical trends (Fig. 1), it might have been

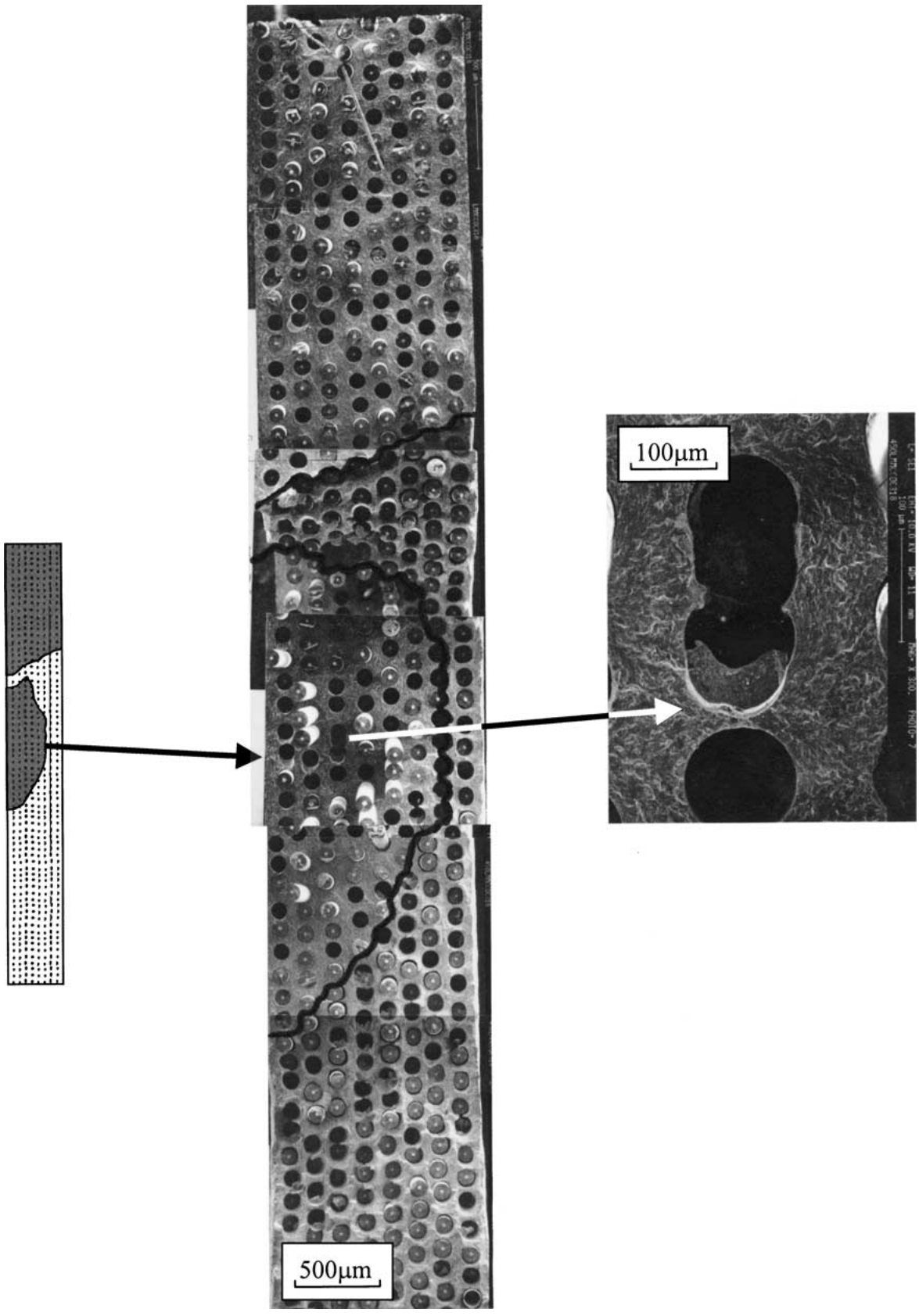

Figure 10 Internally initiated matrix fatigue crack in region III. Note initiation feature.

expected to last for 150,000 cycles. This illustrates the importance of a consistent fibre spacing when designing TMCs against fatigue.

The change in gradient in the strain range versus cycle graphs (Fig. 5a), just before specimen failure, has been observed in SCS-6 reinforced TMCs [22, 35, 39] and is due to the onset of significant fibre failure as indicated by the increase in acoustic activity. The onset of significant fibre failure is due to two mechanisms. Firstly, as the matrix cracks grow, there is less intact matrix to support the load. Thus, the stress in the fibres increases until eventually fibres, both in the bulk and bridging the crack, begin to fail. At elevated temperature the ratchetting of the matrix, which transfers load to the fibres, also contributes to the increase in fibre stress.

4.2. Region II behaviour

Damage development in region II shows no unique mechanism, but rather a mixture of those operating in regions III and I. In this region of the S-N curve, Ti-15-3/SCS-6 has been shown to suffer extensively from matrix cracks initiated internally at fibre/matrix interfaces [8, 21, 26, 37]. In agreement with work on Ti-6-4/SCS-6 [8, 9], however, the current Ti-6-4/SM1140+ shows no such matrix cracking. This is likely to be linked to the strength of the interfacial layers and bond.

Surface initiated matrix cracks are smaller in region II than in region III, and decrease in size as the cyclic stress increases (Fig. 7). Matrix creep becomes the dominant matrix deformation mechanism in region II, and is the major cause of the gradual increase in the cyclic strain range (Fig. 5b). The lack of acoustic emission during the major part of the fatigue test confirms that the increase in cyclic strain range is not due to fibre failure. Matrix creep increases with increasing temperature so that, for a given cyclic stress, fibres will reach the critical stress required for fracture in fewer cycles as the temperature increases. This is the cause of the divergence of the S-N curves in region II (Fig. 1).

The transfer of load to fibres from the creeping matrix eventually leads to the onset of fibre failure. As in region III, this period of fibre failure shortly before specimen fracture is characterised by an increase in the rate of rise in strain range and the onset of significant acoustic emission (Fig. 5b).

4.3. Region I behaviour

In region I, the stress required to produce a given fatigue life decreases dramatically with temperature (Fig. 1).

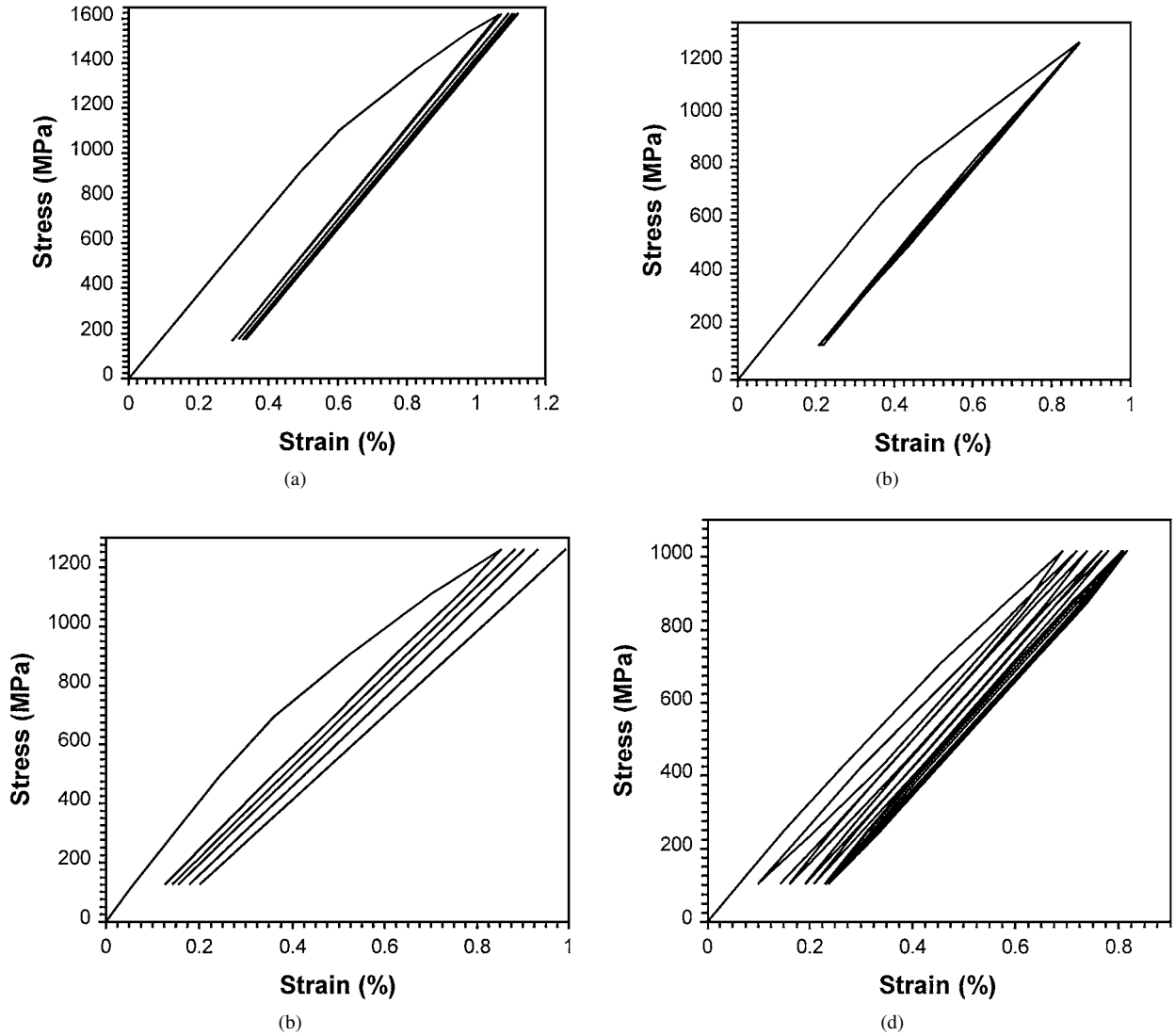

Figure 11 Comparison of cyclic stress-strain curves in Region I of the S-N curve. (a) 22°C; (b) 350°C; (c) 450°C; (d) 600°C.

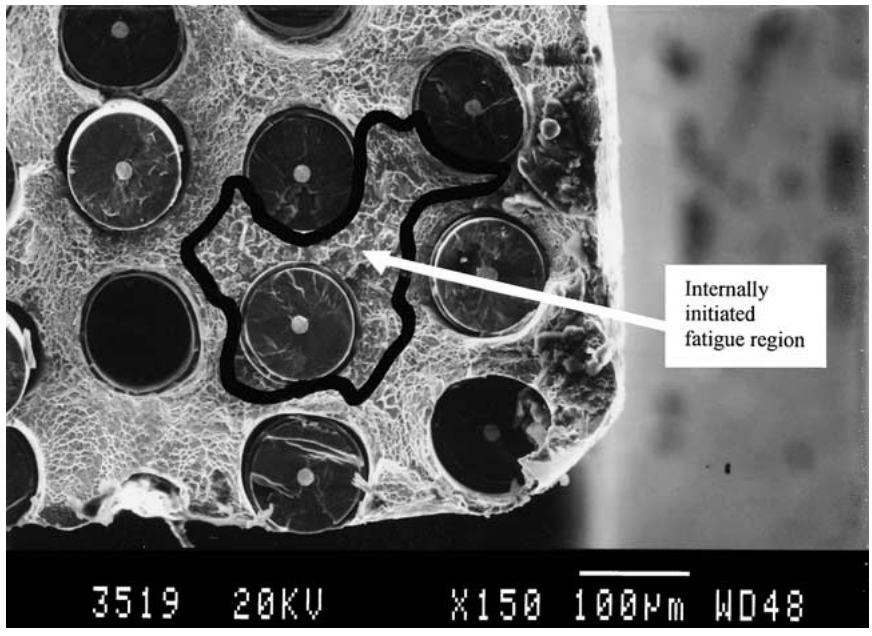

Figure 12 Internally initiated matrix fatigue crack after fatigue in Region I.

Increasing temperature reduces the matrix creep resistance, resulting in the magnitude of ratchetting increasing as temperature increases (Fig. 11) which, in turn, transfers more load to fibres. This, together with a reduction in the compressive residual fibre stress, means that significantly reducing the cyclic stress as temperature increases still results in the fibres reaching their failure stresses after a similar number of cycles.

An acoustic peak occurs near the end of tests, as in regions II and III, indicating a sudden increase in fibre failure immediately before fracture (Fig. 5c). Acoustic emission is relatively high for the whole duration of the tests, however, suggesting that fibre failure is occurring throughout the test at these high stresses. The steep increase in strain range (Fig. 5c) is attributed therefore to matrix creep and fibre failure. The suggestion that specimen failure in region I is due to fibre failure is confirmed when the failure strains of the fatigue specimens (Fig. 11) are compared to failure strains during tensile tests [40]. At room temperature the Ti-6-4/SM1140+ TMC displays a fatigue failure strain of 1.11%, which compares well with a tensile failure strain of 1.08%. As occurs during tensile testing, the strain to failure in the fatigue tests generally decreases with increasing temperature. At 600°C the failure strain in fatigue is 0.81%, which is similar to the failure strain in tension, of 0.90%.

Matrix fatigue cracking is negligible in region I, as observed in other TMCs [8, 15]. Fatigue fracture surfaces have the same appearance as tensile fracture surfaces, with ductile matrix dimpling. Internally initiating fatigue cracks are occasionally observed in region I, but these are both rare, and small (Fig. 12). These matrix cracks have most probably initiated at fibre breaks [12].

5. Conclusions

1. The TMC S-N curve can be split into three distinct regions. The region II and region III fatigue performance of Ti-6-4/SM1140+ is, within the scatter of literature data, the same as that for Ti-6-4/SCS-6. In region I, it is possible that Ti-6-4/SM1140+ has inferior fatigue performance compared to Ti-6-4/SCS-6, as a result of the lower fibre strength.

2. In region I, damage development is via matrix creep and resultant fibre overload.

3. In region III, damage development is primarily by matrix crack growth, followed by matrix creep. Fibre failure only becomes significant near the end of the test as a result of transfer of load.

4. In region II, damage development is a mixture of the mechanisms observed in regions I and III.

5. Matrix fatigue cracks initiate, almost exclusively, at the machined edges of specimens.

6. Poor fibre spacing has been shown to have a deleterious effect on fatigue crack initiation resistance.

Acknowledgements

This work was supported under the MOD Applied Research Programme and DTI CARAD programme. Thanks are due to D. G. P. Martin for help with testing and S. Sweby for help with fractography.

References

1. M. P. THOMAS, J. G. ROBERTSON and M. R. WINSTONE, *J. Mater. Sci.* **33** (1998) 3607.
2. M. P. THOMAS, S. BATE, J. G. ROGERTSON and M. R. WINSTONE, *Mat. Sci. Tech.* **14** (1998) 1009.
3. M. C. MERIENNE and J. P. FAVRE, in Proceedings of the Third International Symposium on Acoustic Emission from Composite Materials-AECM-3 (American Society for Non-Destructive Testing, Ohio, 1989) p. 304.
4. K. TAKASHIMA, K. M. FOX, C. BARNEY, J. G. PURSELL and P. BOWEN, *Mat. Sci. Tech.* **12** (1996) 917.
5. R. L. BRETT, P. J. COTTERILL and P. BOWEN, *Int. J. Fat.* **18** (1996) 1.
6. T. NICHOLAS, M. G. CASTELLI and M. L. GAMBONE, *Scripta Materialia* **36** (1997) 585.
7. S. MALL and T. NICHOLAS in "Titanium Matrix Composites: Mechanical Behavior" (Technomic Publishing, Pennsylvania, 1998) 169.

8. S. M. JENG, P. ALASSEUR, J. M. JANG and S. AKSOY, *Mat. Sci. Eng.* A **148** (1991) 67.
9. I. GREAVES, J. R. YATES and H. V. ATKINSON, *Composites* **25** (1994) 692.
10. E. R. DE LOS RIOS, C. A. RODOPOULOS and J. R. YATES, *Fat. Fract. Eng. Mat. Struct.* **19** (1996) 539.
11. J. H. TWEED, J. COOK, N. L. HANCOCK, R. J. LEE and R. F. PRESTON, in AGARD Report 796, paper 20 (NATO AGARD, France, 1994).
12. B. P. SANDERS, S. MALL and R. B. PITTMAN, *Comp. Sci. Tech.* **59** (1999) 583.
13. S. M. JENG, J. M. YANG and S. AKSOY, *Mat. Sci. Eng.* A **156** (1992) 117.
14. D. D. ROBERTSON, S. MALL and S. M. LEE, *J. Comp. Tech. Res.* **20** (1998) 120.
15. P. LIPETZKY, G. J. DVORAK and N. S. STOLOFF, *Scripta Mater.* **35** (1996) 1089.
16. B. P. SANDERS, S. MALL and S. C. JACKSON, *Int. J. Fat.* **21** (1999) 121.
17. A. VASSEL, F. PAUTONNIER and M. H. VIDAL-SETIF, in "Test Techniques for Metal Matrix Composites" (Institute of Physics, Bristol, 1991) p. 55.
18. Y. LEPETITCORPS, M. LAHAYE, R. PAILLER and R. NASLAIN, *Comp. Sci. Tech.* **32** (1988) 31.
19. R. A. SHATWELL, *Mat. Sci. Tech.* **10** (1994) 552.
20. S. Q. GUO, Y. KAGAWA, Y. TANAKA and C. MASUDA, *Acta Mater.* **46** (1998) 4941.
21. W. O. SOBOYEJO, B. M. RABEETH and P. KANTZOS, *Mat. Sci. Eng.* **A200** (1995) 140.
22. B. S. MAJUNDAR and G. M. NEWAZ, *Phil. Mag.* A **66** (1992) 187.
23. R. T. BHATT and H. H. GRIMES, *Met. Trans.* **13A** (1982) 1933.
24. B. P. SANDERS and S. MALL, *J. Comp. Tech. Res.* **16** (1994) 304.
25. Y. TANAKA, Y. KAGAWA, C. MASUDA, Y. F. LIU and S. Q. GUO, *Met. Trans.* **30A** (1999) 221.
26. T. P. GABB, J. GAYDA and R. A. MACKAY, *J. Comp. Mat.* **24** (1990) 667.
27. M. P. THOMAS and M. R. WINSTONE, *Comp. Sci. Tech.* **59** (1999) 297.
28. T. P. GABB, J. GAYDA, B. A. LERCH and G. R. HALFORD, *Scripta Metall.* **25** (1991) 2879.
29. M. P. THOMAS, Composite Science and Technology, in press.
30. A. FUKUSHIMA, C. FUJIWARA, Y. KAWACHI and K. YASUHIRA, in Proceedings of ICCM-12: Twelfth International Conference on Composite Materials, CD ROM Proceedings (ICCM12/TCA, Paris, 1999).
31. J. GAYDA, T. P. GABB and B. A. LERCH, *Int. J. Fat.* **15** (1993) 41.
32. D. P. WALLS, G. BAO and F. W. ZOK, *Acta Metall.* **41** (1993) 2061.
33. D. D. ROBERTSON and S. MALL, in Proceedings of ICCM-11: Eleventh International Conference on Composite Materials, CD ROM Proceedings, edited by M. L. Scott (Australian Composite Structures Society, Melbourne, 1997) Vol. 3, p. 317.
34. D. HARMON, K. L. JERINA and S. M. L. SASTRY, *J. Comp. Mat.* **31** (1997) 534.
35. D. L. KRAABEL, B. P. SANDERS and S. MALL, *Comp. Sci. Tech.* **57** (1997) 99.
36. B. S. MAJUMDAR and G. M. NEWAZ, *Mat. Sci. Eng.* A **200** (1995) 114.
37. P. C. WANG, S. M. JENG and J. M. YANG, *ibid.* A **200** (1995) 173.
38. S. G. WARRIER, B. MARUYAMA, B. S. MAJUMDAR and D. B. MIRACLE, *ibid.* **A259** (1999) 189.
39. T. NICHOLAS and S. M. RUSS, *ibid.* A **153** (1992) 514.
40. M. P. THOMAS and M. R. WINSTONE, *Scripta Materialia* **37** (1997) 1855.

Received 4 April 2000
and accepted 27 March 2002